ACS chemical biology

Articles

pubs.acs.org/acschemicalbiology

A Liver-Selective LXR Inverse Agonist That Suppresses Hepatic Steatosis

Kristine Griffett, Laura A. Solt, Bahaa El-Dien M. El-Gendy, Theodore M. Kamenecka, and Thomas P. Burris*

The Scripps Research Institute, Jupiter, Florida 33458, United States

Supporting Information

ABSTRACT: Fatty liver, which often accompanies obesity and type 2 diabetes, frequently leads to a much more debilitating hepatic disease including non-alcoholic steatohepatitis, cirrhosis, and hepatocellular carcinoma. Current pharmacological therapies lack conclusive efficacy and thus treatment options are limited. Novel therapeutics that suppress either hepatic lipogenesis and/or hepatic inflammation may be useful. Here, we describe the development of the first selective synthetic LXR inverse agonist (SR9238) and demonstrate that this compound effectively suppresses hepatic lipogenesis, inflammation, and hepatic lipid accumulation in a mouse model of non-alcoholic hepatosteatosis. SR9238 displays high potency for both LXRα and LXRβ (40−200 nM IC_{50}) and was designed to display liver specificity so as to avoid potential side effects due to suppression of LXR in the periphery. Unexpectedly, treatment of diet-induced obese mice with SR9238 suppressed plasma cholesterol levels. These data indicate that liver-selective LXR inverse agonists may hold utility in the treatment of liver disease.

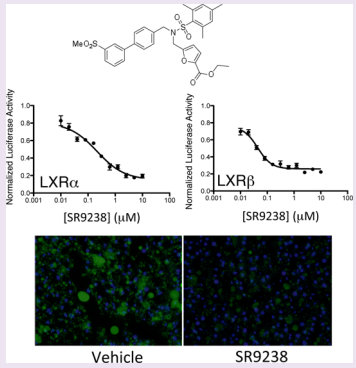

Non-alcoholic fatty liver disease (NAFLD) accompanies metabolic syndrome, comprises a wide spectrum of disorders from a fatty liver (non-alcoholic hepatosteatosis) to the more aggressive non-alcoholic steatohepatitis (NASH), cirrhosis, and hepatocellular carcinomas (HCC), and affects millions of people worldwide. NAFLD affects between ∼14−30% of the general population.[1,2] Current treatment options such as lifestyle changes focusing on alteration of diet and weight loss are inadequate for a large number of patients. Pharmacological therapies such as insulin sensitizers, antioxidants, and lipid-lowering agents display only limited efficacy.[3] There is a clear unmet medical need for development of new pharmacological therapies that limit hepatic steatosis and progression of the disease into NASH as well as even more severe hepatic disease.

NAFLD is associated with insulin resistance that promotes *de novo* lipogenesis and inhibits fatty acid oxidation leading to excessive accumulation of triglycerides in the liver.[4,5] Much of the excessive fat accumulation in the liver is associated with increased lipogenesis due to increased expression of lipogeneic enzymes driven by excessive sterol regulatory element binding protein 1c (SREBP-1c) and carbohydrate responsive element-binding protein (ChERBP) activity.[5] We hypothesized that either blocking activation of lipogenic enzyme expression or active suppression of these genes in the liver would be one method to treat NAFLD. In order to accomplish this, we focused on the nuclear receptors liver X receptor α and β (LXRα and LXRβ) that are well-characterized regulators of the expression of an array of lipogenic enzyme genes.[6] LXR agonists induce lipogenesis by increasing transcription of lipogenic enzyme gene expression including *Srebf1*, *fatty acid synthase* (*Fasn*), *stearoyl-CoA desaturase* (*Scd1*), and *Chrebp*.[7−10] In fact, LXRα expression as well as lipogenic LXRα target genes are overexpressed in patients with NAFLD.[11] A number of synthetic LXR agonists have been designed,[12] but there are limited examples of antagonists.

RESULTS AND DISCUSSION

We hypothesized that a LXR inverse agonist that actively recruits transcriptional corepressor to target gene promoters would be effective at actively silencing genes involved in lipogenesis. Using a recently described tertiary sulfonamide LXR antagonist chemical scaffold as a point of initiation,[13] we developed compounds that effectively recruited corepressor proteins in biochemical assays and optimized compounds for this activity. One compound in particular, SR9238 (Figure 1a; Supplementary Figure 1), displayed very potent inverse agonist activity in cell-based cotransfection assays using either full-length LXRα or LXRβ and a reporter containing 3 copies of an LXRE within the promoter (Figure 1b). SR9238 displayed a degree of LXRβ selectivity with an IC_{50} of 214 nM for LXRα and 43 nM for LXRβ. SR9238 displayed no activity at any of the NRs tested (Figure 1c). SR9238 also effectively suppressed transcription from a *Fasn* promoter driven luciferase reporter (Figure 1d). On the basis of this activity, we hypothesized that SR9238 must be inducing a conformation within the receptor allowing for effective recruitment of corepressor. This was indeed the case as we found that SR9238 induced increased interaction of CoRNR box peptides derived from NCoR (NCoR ID1 and NCoR ID2) with both LXRα and LXRβ, while causing decreased interaction with a

Received: October 4, 2012
Accepted: December 11, 2012
Published: December 13, 2012

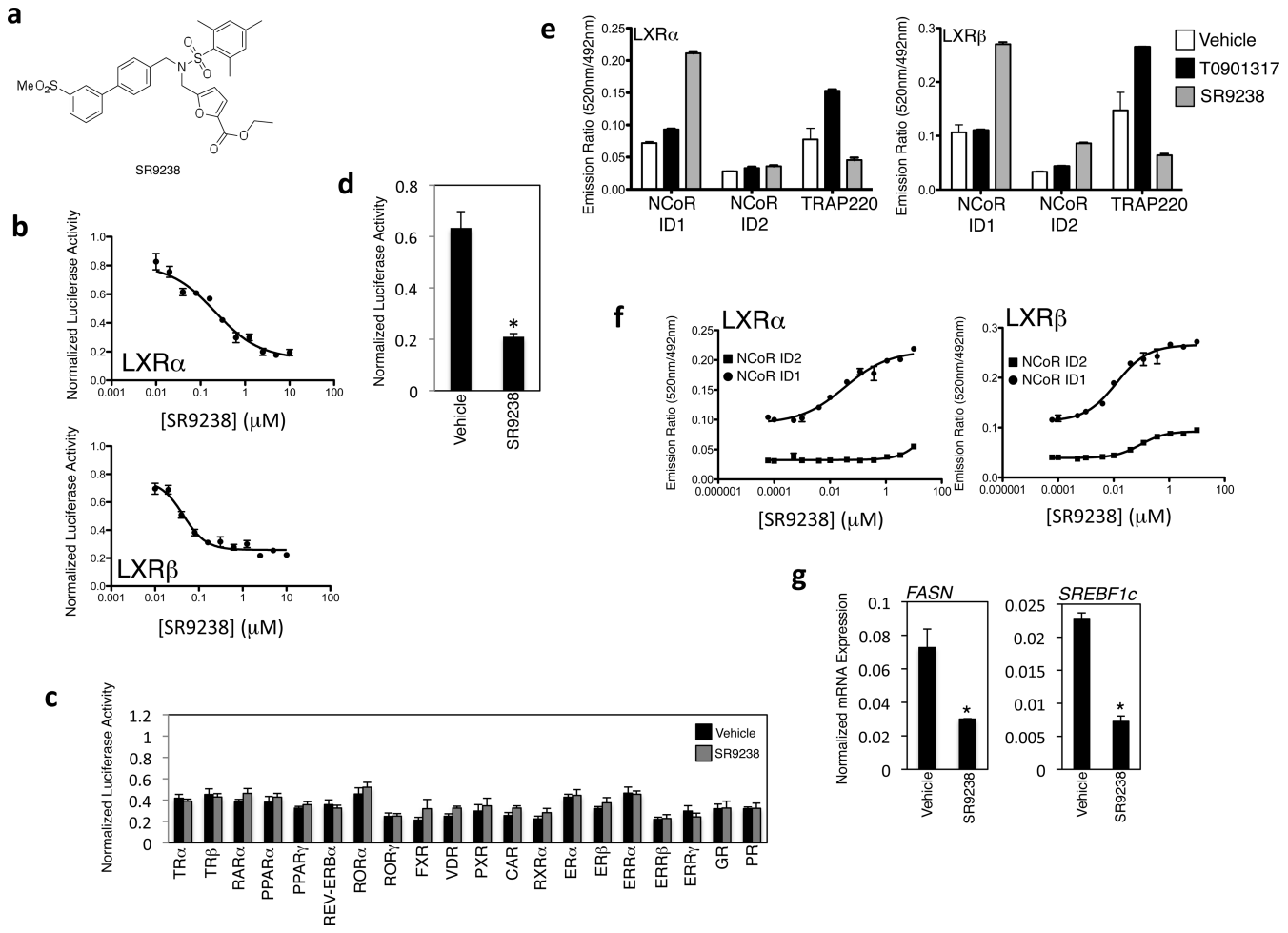

Figure 1. Characterization of SR9238, a LXR inverse agonist. (a) Structure of the LXR inverse agonist SR9238. (b) A cell-based cotransfection assay using a LXR responsive luciferase reporter illustrates the ability of SR9238 to suppress basal transcriptional activity of both LXRα and LXRβ in HEK293 cells. IC_{50} values were 214 and 43 nM for LXRα and LXRβ, respectively. (c) Nuclear receptor specificity panel illustrating the specificity of SR9238. A Gal4-NR LBD cell-based cotransfection assay was utilized. Data was analyzed by ANOVA followed by Tukey's post hoc test. * indicates $p < 0.05$ (d) Full-length LXRα cotransfection assay performed in HEK293 cells demonstrates the ability of SR9238 (10 μM) to suppress basal transcription driven by the *FAS* promoter. (e) Biochemical interaction assay displaying the ability of SR9238 to induce interaction of LXRα and LXRβ with CoRNR box peptides derived from NCoR. Compounds were utilized at a concentration of 10 μM. (f) Time-resolved fluorescent resonance energy transfer biochemical nuclear receptor−corepressor interaction assay assay illustrating the SR9238 dose-responsiveness of recruitment of CoRNR box peptides (box = NCoR ID2 peptide, circle = NCoR ID1 peptide) to LXRα and LXRβ. (g) SR9238 suppresses *FASN* and *SREBP1c* mRNA expression in HepG2 cells. HepG2 cells incubated in the presence of insulin were treated with SR9238 (10 μM) for 1 day followed by assessment of *FASN* and *SREBP1c* mRNA expression by QPCR. mRNA expression was normalized to GAPDH expression. * indicates $p < 0.05$ using Student's *t* test. All luciferase assays were normalized using the Dual-Glo system with renilla luciferase.

coactivator NR box peptide derived from TRAP220 (Figure 1e). As a control, the LXR agonist T0901317 was used to illustrate the ability of an agonist-induced interaction of LXRα and LXRβ with a NR box peptide but not with a CoRNR box peptide (Figure 1f and Supplemental Figure 2). SR9238-induced recruitment of CoRNR box peptides was dose-dependent for both LXRα and LXRβ (Figure 1e). There was a clear preference for NCoR ID1 for both LXRα and LXRβ with EC_{50}'s of 33 and 13 nM for NCoR ID1 with LXRα and LXRβ, respectively, and >10 μM and 93 nM for NCoR ID2 with LXRα and LXRβ, respectively. Furthermore, when we treated HepG2 cells with SR9238 we found that *Fasn* and *Srebp1c* mRNA expression was substantially suppressed (Figure 1g).

One significant concern with development of LXR inverse agonists for the treatment of fatty liver disease is that suppression of LXR target genes outside the liver may have adverse effects on reverse cholesterol transport *via* suppression of ATP-binding cassette transporter subfamily A1 (Abca1) expression for example. LXR agonists have been demonstrated to increase reverse cholesterol transport *via* increased extra-hepatic Abca1 expression.[14−16] We utilized an approach where the LXR inverse agonist would be rapidly metabolized in the liver so as to provide extensive liver exposure, but not peripheral plasma exposure. As illustrated in Figure 2a, SR9238 contains an ester group that we expected to be rapidly metabolized to the acid analogue (SR10389) by plasma lipases. SR10389 displays no LXRα or LXRβ activity in the cell-based cotransfection assay (Figure 2b). In order to confirm that there would be liver exposure but no plasma exposure, we injected SR9238 (30 mg/kg, ip) into mice and assessed the concentration of SR9238. Approximately 6 μM SR9238 was detected in the liver 2h after the injection, but no compound was detected in the plasma (Figure 2c). In a separate experiment, we injected mice once per day for 3 consecutive days with SR9238 and assessed SR9238 levels. As shown in Figure 2d, we detected

dx.doi.org/10.1021/cb300541g | *ACS Chem. Biol.* 2013, 8, 559−567

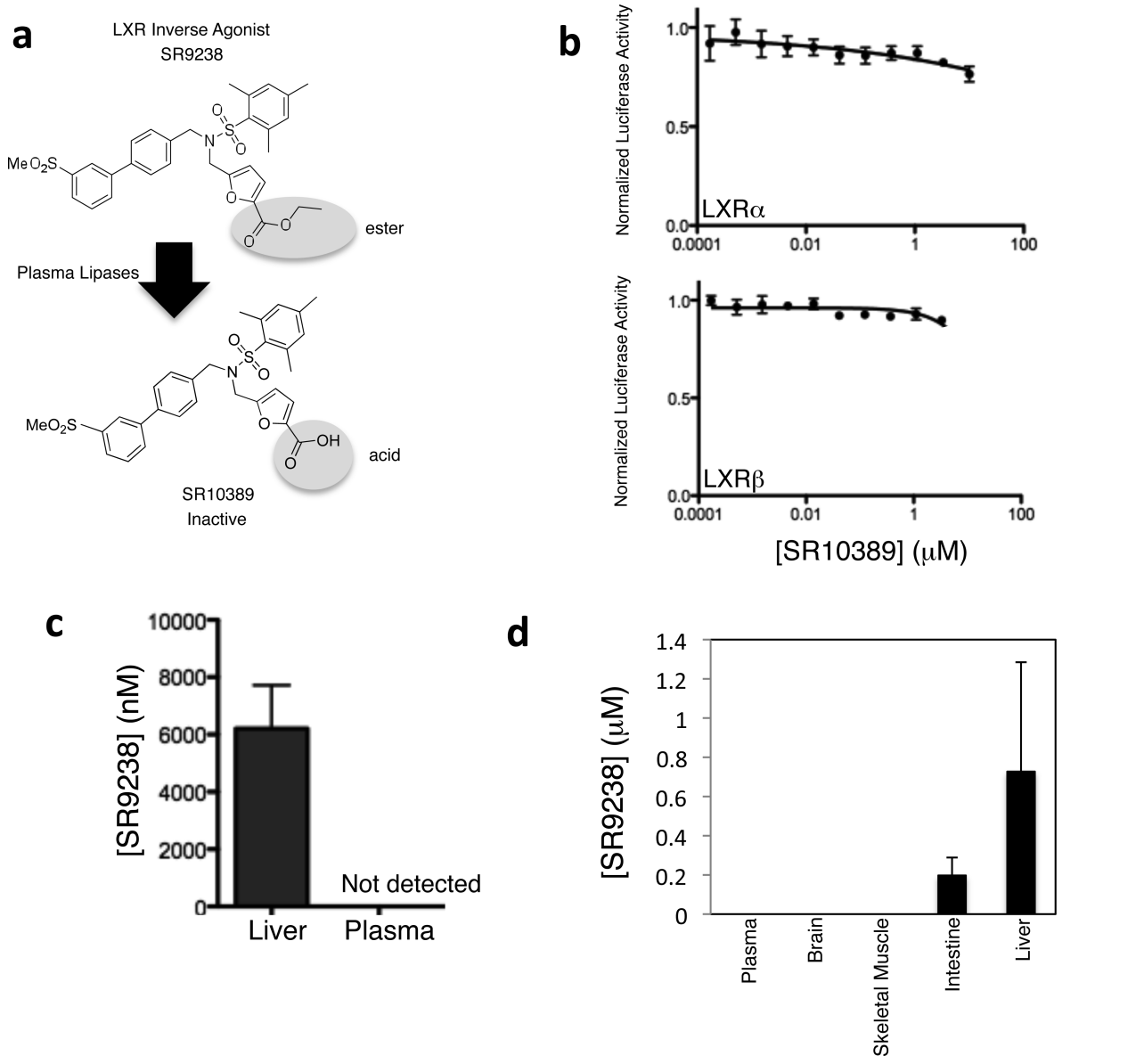

Figure 2. The acid analogue of SR9238 displays no LXR activity and has significant liver exposure with no plasma exposure. (a) Schematic showing the predicted cleavage of the ester group of SR9238 to the acid analogue, SR10389. (b) SR10389 was synthesized and tested for activity in the LXR cotransfection assay. As indicated in the figure, activity was not observed in this assay. (c) Pharmacokinetic data illustrating that SR9238 displays significant liver exposure but no plasma exposure following a single injection (30 mg/kg, ip). Levels were assessed by mass spectroscopy 2 h after treatment. (d) Pharmacokinetic data illustrateing that SR9238 displays liver and intestinal exposure but no plasma, skeletal muscle, or brain exposure after 3 days of dosing (30 mg/kg ip once per day).

high levels in the liver. We also detected SR9238 in the intestine as would be expected with either ip or oral administration. However, no SR9238 was detectable in the plasma, skeletal muscle, or brain, consistent with SR9238 not surviving first pass metabolism. Thus, SR9238 displays liver-specific exposure and would not be expected to alter LXR target gene expression outside of the liver.

In order to determine the potential of SR9238 to treat fatty liver disease, we induced hepatic steatosis in mice by maintaining them on a high fat diet for 14 weeks prior to initiating treatment with SR9238 (30 mg/kg/day, ip) for 30 days. Consistent with our cell-based data, we found that SR9238 treatment resulted in the substantial repression of lipogenic gene expression. Hepatic *Fasn* and *Srebp1c* expression was suppressed by 60% and 80%, respectively (Figure 3a). Additionally, *Scd1* was reduced almost 90% following the treatment (Figure 3a). Hepatic steatosis was assessed by visualization of lipid content in liver sections stained with Bodipy 493/503 (Figure 3b) and quantitated (Figure 3c). Clearly, SR9238-treated mice displayed greatly reduced lipid content in the liver (Figure 3b and c). Several studies suggest that the increased expression of *Srebp1c* together with other lipogenic genes and the induction of inflammation in hepatocytes are crucial for the development and progression of fatty liver diseases.[11,17,18] To assess whether SR9238 also impacted inflammation due to the hepatic steatosis, the expression of *Tnfa* and *Il1b* was examined. As illustrated in Figure 3d, both *Tnfa* and *Il1b* expression were substantially reduced (~80% and >95%, respectively) in the SR9238-treated mice when compared to the vehicle-treated mice. Kupffer cells (liver resident macrophages) have been suggested to play a critical role in the etiology of NASH as they are the first cell to

dx.doi.org/10.1021/cb300541g | *ACS Chem. Biol.* 2013, 8, 559–567

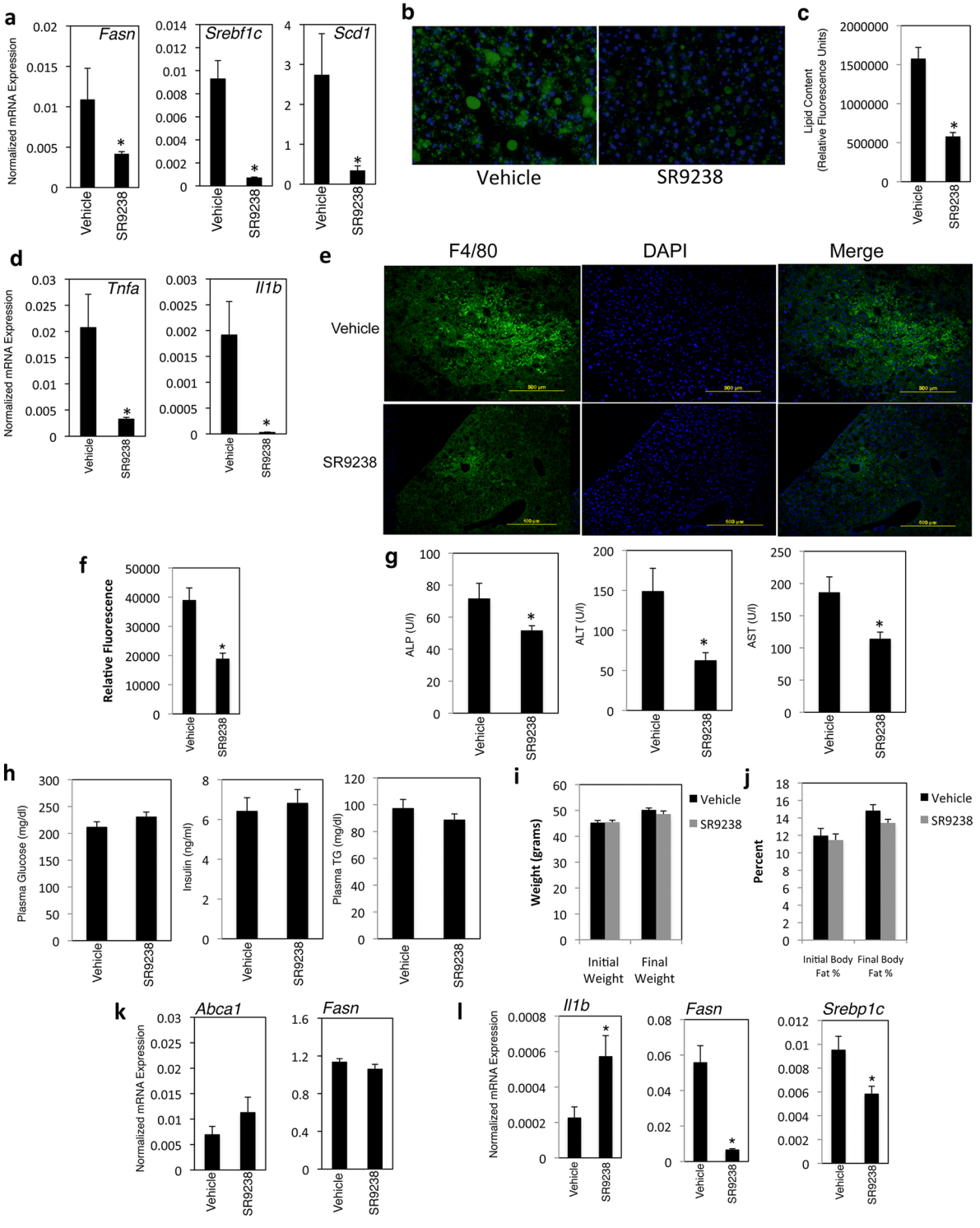

Figure 3. SR9238 suppresses the expression of lipogenic enzyme and proinflammatory cytokine genes in an animal model of hepatic steatosis. (a) Gene expression analysis of the livers of DIO mice ($n = 7$) following a 1-month treatment with SR9238. (b) Liver sections stained with Biodipy 493/503 to identify lipids and counterstained with DAPI to identify the nuclei. (c) Quantitation of lipid content in the liver of the DIO mice following vehicle or SR9238 treatment. (d) Gene expression analysis of inflammation markers from liver tissue of DIO mice following a 1-month treatment with SR9238. (e) Staining of liver sections (DIO mice) with anti-F4/80 to quantitate Kupffer cell infiltration in response to vehicle or SR9238 treatment. DAPI staining of the nuclei is also illustrated along with the merged image. Bar indicates 500 μm. (f) Relative fluorescence of F4/80 staining taken from liver sections as described in panel e illustrating a reduction in F4/80 staining in SR9238 treated mice. (g) Markers of hepatocellular injury in the plasma following 1-month treatment of DIO mice with vehicle or SR9238. (h) Plasma glucose, insulin, and triglycerides (TG) in DIO mice following a 1-month treatment with SR9238. (i) Body weight of DIO mice prior to initiation of treatment and post SR9238 treatment. (j) Percentage body fat composition of DIO mice prior to treatment and post SR9238 treatment. (k) Gene expression analysis of the brown adipose tissue of treated DIO mice. (l) Hepatic expression of *Il1b*, *Fasn*, and *Srebp1c* in mice fed a normal chow diet treated with vehicle or SR9238 for 7 days. mRNA expression was normalized to GAPDH expression. * indicates $p < 0.05$ using Student's t test.

dx.doi.org/10.1021/cb300541g | *ACS Chem. Biol.* 2013, 8, 559–567

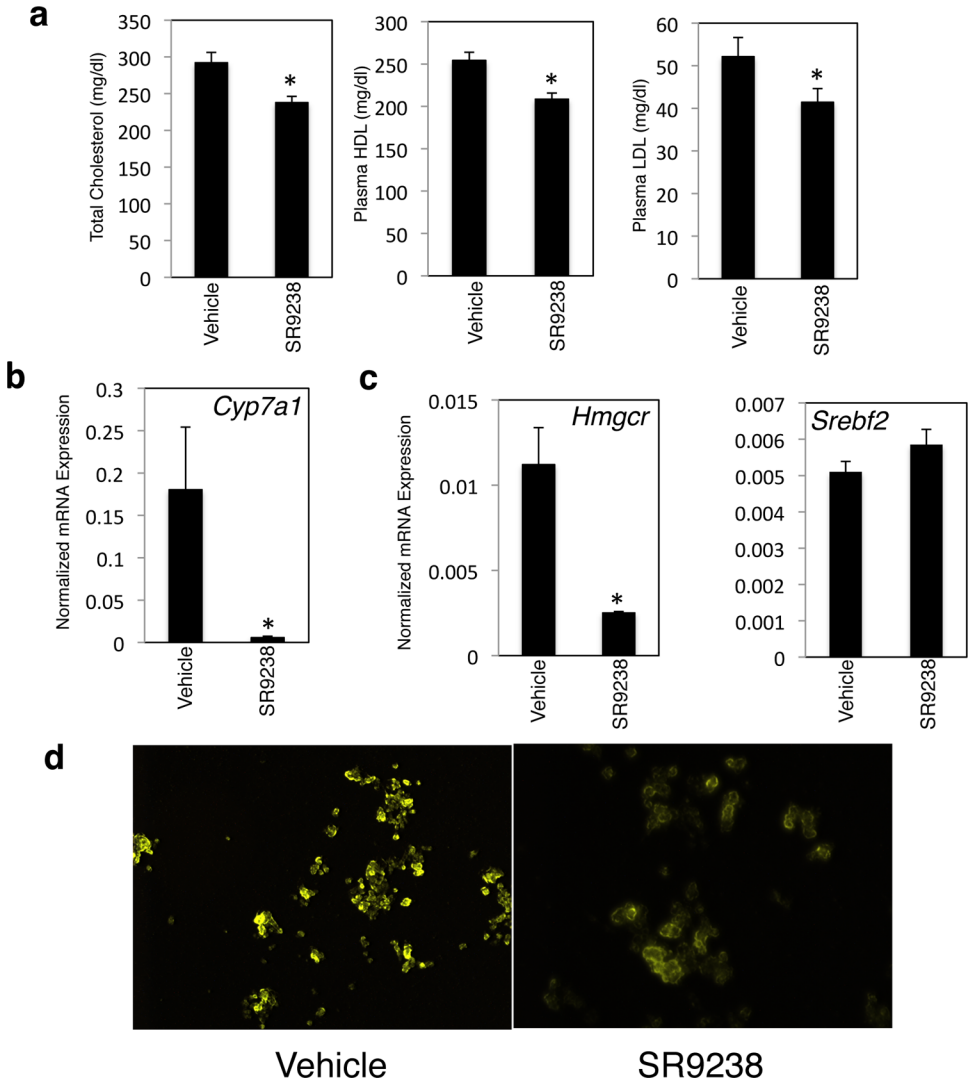

Figure 4. SR9238 treatment decreases plasma cholesterol levels. (a) Plasma total cholesterol, HDL and LDL levels in DIO mice following a 1-month treatment with vehicle or SR9238. (b). Hepatic *Cyp7a1* mRNA expression following 1-month treatment in the DIO mice. (c) Hepatic *Hmgcr* and *Srebf 2* mRNA expression following 1-month treatment in the DIO mice. (d) Assessment of cellular localization of SREBP2 following vehicle or SR9238 treatment in HepG2 cells. * indicates $p < 0.05$ using Student's *t* test.

respond to hepatocyte injury leading to increased TNFα secretion.[19] Due to the critical role of these cells in development of NASH, we assessed the relative number of Kupffer cells in the liver by immunohistochemistry (F4/80 staining). As illustrated in Figure 3e, SR9238-treated DIO mice displayed considerably lower intensity of F4/80 staining (Figure 3f) versus vehicle-treated DIO mice consistent with a beneficial effect of SR9238 on NASH. We also assessed markers of hepatocellular injury (alkaline phosphatase (ALP), alanine transaminase (ALT), and aspartate aminotransferase (AST)) and found that SR9238 treatment reduced these markers substantially (Figure 3g). We noted no alteration in plasma glucose, plasma insulin, or plasma triglyceride levels in the mice (Figure 3h). SR9238 treatment did not alter body weight or percent body fat composition relative to vehicle treated animals during the experiment (Figure 3i and j). On the basis of the pharmacokinetic data showing that SR9238 exposure was limited in the liver (Figure 2c and d), we expected that there would be no alterations in LXR target genes in other tissues. We assessed *Fasn* and *Abca1* expression in brown adipose tissue (a well-characterized LXR target tissue[20−22]) of the DIO mice and observed no significant changes in expression levels following 30-day treatment with SR9238 (Figure 3k). Thus, treatment with the LXR inverse agonist, SR9238, suppresses diet-induced hepatosteatosis, hepatic inflammation, and hepatocellular injury. Given that LXR activity is generally considered anti-inflammatory,[23,24] one might expect that a LXR inverse agonist would be proinflammatory. However, we hypothesized that an agent that significantly suppresses lipid accumulation and the accompanying massive inflammatory response to these lipids in NASH may have efficacy even if it displayed some intrinsic proinflammatory activity. In order to test this, we treated chow fed mice for 7 days (30 mg/kg, ip) and examined hepatic expression of *Il1b*. As shown in Figure 3l, we did observe a significant increase in this pro-inflammatory cytokine while also observing a concomitant decrease in the expression of lipogenic genes, *Fasn* and *Srebp1c*. These data suggest that while SR9238 may initially be pro-inflammatory, long-term use counters this response (at least in the context of a highly inflammatory NASH model). Thus, decreasing hepatic lipid accumulation, which induced a pro-inflammatory environment in the first place, is of

dx.doi.org/10.1021/cb300541g | *ACS Chem. Biol.* 2013, 8, 559−567

greater consequence than the initial pro-inflammatory response induced by SR9238. Regardless, this type of compound would not likely be given short-term to normal, healthy individuals, and our data clearly indicate that the net effect on hepatic inflammation in mice with NASH is anti-inflammatory.

LXR plays an important role in cholesterol elimination where elevated levels of oxysterol cholesterol metabolites upregulate the rate-limiting enzyme in bile acid production, cholesterol 7α hydroxylase (Cyp7a1), to allow for greater conversion of cholesterol to bile acids.[25,26] In fact, in high cholesterol diet fed LXRα null mice there is massive hepatic accumulation of cholesterol due to the inability of the mice to upregulate *Cyp7a1* expression and eliminate cholesterol.[26] These mice also display an elevation in plasma LDL.[26,27] LXRβ null mice display resistance to this effect suggesting that LXRα plays the dominant role in regulation of *Cyp7a1* in response to elevated cholesterol levels.[27] On the basis of these observations, we anticipated that treatment of the DIO mice with SR9238 might have deleterious effects on cholesterol metabolism. Unexpectedly, we observed that total plasma cholesterol, plasma LDL, and plasma HDL levels were all reduced in SR9238-treated mice (Figure 4a). This decrease was despite massively reduced *Cyp7a1* expression (Figure 4b), suggesting that there must be reduced cholesterol synthesis. This indeed appears to be the case since expression of the gene for the rate-limiting enzyme HMG CoA reductase (*Hmgcr*) was suppressed by 80% (Figure 4c). There has been no reported regulation of the *Hmgcr* gene by LXR, thus we considered proteins that regulate *Hmgcr* expression such as SREBP1a and SREBP2. LXR does not regulate *Srebp1c* expression,[10,28] and we examined expression of *Srebf2* and found that there was no effect (Figure 4c). We also considered the possibility that treatment with SR9238 altered the proteolytic processing of SREBP1a/SREBP2 thus regulating their activity. The activities of the SREBPs are tightly regulated by proteolytic processing and in the inactive state the SREBPs are transmembrane proteins found in the endoplasmic reticulum. Proteolytic cleavage of the SREBPs yields functional transcription factors and is dependent on the cellular sterol levels. When sterol levels are depleted, cleavage occurs allowing for SREBP1a and SREBP2 translocation to the nucleus where they activate the expression of a number of genes in the cholesterol biosynthetic pathway.[29,30] In order to test the possibility that SR9238 altered SREBP processing, we assessed the cellular localization of SREBP2 by immunocytochemistry in HepG2 cells. We observed a very prominent effect of SR9238 on SREBP2 translocation where the LXR inverse agonist blocked the constitutive nuclear localization of SREBP2 in HepG2 cells (Figure 4d) suggesting that this compound interferes with its processing. Thus, the effect of SR9238 on *Hmgcr* expression may be due to decreased SREBP2 activity.

We have developed a high affinity, liver-selective LXR inverse agonist that displays the ability to reduce the expression of lipogenic genes in the liver as well as reduce hepatic steatosis in obese mice. In addition, SR9238 reduces the expression of pro-inflammatory cytokines and reduces markers of hepatocellular injury in the hepatic steatosis model. Unexpectedly, SR9238 reduces plasma cholesterol levels, likely *via* reduction of cholesterol synthesis due to an 80% reduction in *Hmgcr* expression. The effect on *Hmgcr* may be indirect due to the ability of SR9238 to reduce SREBP2 translocation to the nucleus. The mechanism by which SR9238 completes this action is unclear and may be due to either SR9238 directly mimicking high levels of sterols thus limiting SREBP2 processing or by altering endogenous oxysterol levels *via* suppression of LXR activity. However, it appears unlikely that SR9238 mimics the action of sterols in the endoplasmic reticulum since SR9238 does not share structural similarities with sterols. Collectively, these data suggest that this new class of compound may be effective in limiting the progression of NAFLD to liver failure and cancer.

METHODS

Synthesis of SR9238 and SR10389.

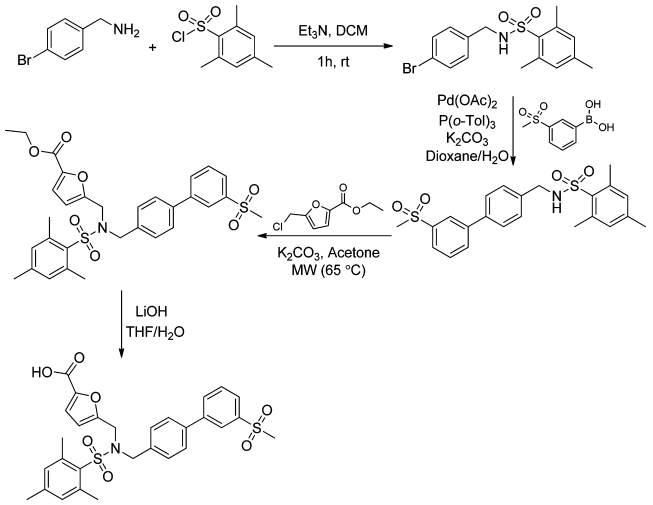

N-(4-Bromobenzyl)-2,4,6-trimethylbenzenesulfonamide.

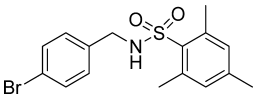

To a solution of (4-bromophenyl)methanamine (0.93 g, 5 mmol) and triethyl amine (1.05 mL, 7.5 mmol) in dichloromethane was added 2,4,6-trimethylbenzene-1-sulfonyl chloride (1.09 g, 5 mmol) portionwise. The mixture was allowed to stir for 1 h at ambient temperature. The reaction mixture was washed with HCl (2 N) (3 × 50 mL), water, and brine. The organic layer was dried over anhydrous $MgSO_4$ and concentrated *in vacuo* to obtain the title compound as colorless prisms; ^{1}H NMR (400 MHz, chloroform-*d*) δ (ppm) 7.38−7.32 (m, 2H), 7.07−7.01 (m, 2H), 6.94 (s, 2H), 4.90 (t, J = 6.2 Hz, 1H), 4.03 (d, J = 6.2 Hz, 2H), 2.61 (s, 6H), 2.31 (s, 3H); ^{13}C NMR (100 MHz, chloroform-*d*) δ (ppm) 142.6, 139.2, 135.6, 133.7, 132.1, 131.8, 129.6, 121.9, 46.3, 23.1, 21.1; HRMS calculated for $C_{16}H_{18}BrNO_2S$ $(M + H)^+$ 368.0314, found 368.0319.

2,4,6-Trimethyl-N-((3′-(methylsulfonyl)-[1,1′-biphenyl]-4-yl)-methyl)benzenesulfonamide.

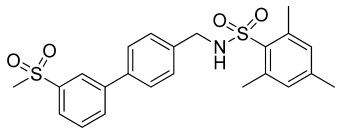

N-(4-Bromobenzyl)-2,4,6-trimethylbenzenesulfonamide (0.736 g, 2 mmol), (3-(methylsulfonyl)phenyl)boronic acid (0.800 g, 4 mmol), palladium acetate (0.044 g, 0.2 mmol), and tri-*o*-tolylphosphine (0.121 g, 0.4 mmol) were dissolved in 1,4-dioxane (50 mL), and the solution was degassed with argon for 10 min. K_2CO_3 (2 M) was added, and the solution was further degassed for additional 5 min. The reaction mixture was heated overnight at 120 °C in an oil bath. After the mixture was cooled to RT, it was poured into aq NaCl (5%) and extracted with dichloromethane (4 × 50 mL). The combined organics were washed with water, dried over anhydrous $MgSO_4$, and concentrated *in vacuo*. The remaining crude residue was purified by flash chromatography on silica gel (ethyl acetate/hexanes) to obtain the title compound as white sharp needles; ^{1}H NMR (400 MHz, chloroform-*d*) δ (ppm) 8.10 (t, J = 1.8 Hz, 1H), 7.91 (ddd, J = 7.8, 1.9, 1.1 Hz, 1H), 7.82 (ddd, J = 7.8, 1.9, 1.1 Hz, 1H), 7.64 (t, J = 7.8 Hz, 1H), 7.55−7.48 (m, 2H), 7.33−7.27 (m, 2H), 6.99−6.94 (m, 2H), 4.81 (t, J = 6.2 Hz, 1H), 4.15 (d, J = 6.2 Hz, 2H),

dx.doi.org/10.1021/cb300541g | *ACS Chem. Biol.* 2013, 8, 559−567

3.09 (s, 3H), 2.66 (s, 6H), 2.31 (s, 3H) ; ^{13}C NMR (100 MHz, chloroform-*d*) δ (ppm) 142.5, 142.1, 141.3, 139.2, 138.6, 137.0, 133.7, 132.2, 132.1, 130.0, 128.7, 127.5, 126.2, 125.8, 46.5, 44.6, 23.1, 21.0; HRMS calculated for $C_{23}H_{25}NO_4S_2$ $(M + H)^+$ 444.1297, found 444.1297.

Ethyl 5-((2,4,6-Trimethyl-N-((3′-(methylsulfonyl)-[1,1′-biphenyl]-4-yl)methyl)phenylsulfonamido)methyl)furan-2-carboxylate. A mix-

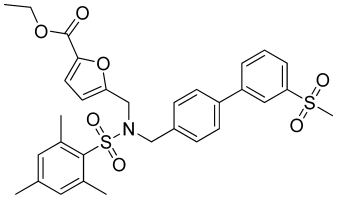

ture of 2,4,6-trimethyl-*N*-((3′-(methylsulfonyl)-[1,1′-biphenyl]-4-yl)-methyl)benzenesulfonamide (0.443 g, 1 mmol), K_2CO_3 (0.276 g, 2 mmol), and ethyl 5-(chloromethyl)furan-2-carboxylate (0.566 g, 3 mmol) in anhydrous acetone (5 mL) was heated to 65 °C for 2 h under microwave irradiation. The mixture was filtered and then concentrated in vacuo. The resulting oil was dissolved in ethyl acetate and washed with brine, dried over anhydrous $MgSO_4$, filtered, and concentrated *in vacuo*. The remaining crude residue was purified by flash chromatography on silica gel (ethyl acetate/hexanes) to obtain the title compound as white sharp needles; ^{1}H NMR (400 MHz, chloroform-*d*) δ 8.12 (t, J = 1.8 Hz, 1H), 7.92 (ddd, J = 7.8, 1.9, 1.1 Hz, 1H), 7.84 (ddd, J = 7.8, 1.8, 1.1 Hz, 1H), 7.64 (t, J = 7.7 Hz, 1H), 7.57−7.51 (m, 2H), 7.29−7.26 (m, 2H), 7.04 (d, J = 3.4 Hz, 1H), 7.02−6.98 (m, 2H), 6.28 (d, J = 3.4 Hz, 1H), 4.40 (s, 2H), 4.35 (q, J = 7.1 Hz, 2H), 4.31 (s, 2H), 3.10 (s, 3H), 2.65 (s, 6H), 2.33 (s, 3H), 1.38 (t, J = 7.1 Hz, 3H); ^{13}C NMR (100 MHz, chloroform-*d*) δ (ppm) 158.6, 154.4, 144.6, 143.1, 142.3, 141.4, 140.6, 138.8, 135.7, 132.8, 132.3, 132.2, 130.1, 129.9, 127.6, 126.2, 125.9, 118.7, 111.4, 61.1, 50.1, 44.7, 41.6, 23.0, 21.2, 14.5; HRMS calculated for $C_{31}H_{33}NO_7S_2$ $(M + H)^+$ 596.1771, found 596.1763.

5-((2,4,6-Trimethyl-N-((3′-(methylsulfonyl)-[1,1′-biphenyl]-4-yl)-methyl)phenylsulfonamido)-methyl)furan-2-carboxylic Acid. To a

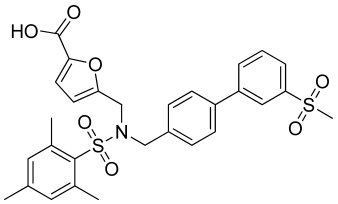

solution of ethyl 5-((2,4,6-trimethyl-*N*-((3′-(methylsulfonyl)-[1,1′-biphenyl]-4-yl)methyl)phenylsulfonamido)methyl)furan-2-carboxylate (0.059 g, 0.1 mmol) in THF (5 mL) and water (2 mL) was added lithium hydroxide monohydrate (0.006 g, 0.25 mmol), and the reaction was stirred at RT for 12 h. The reaction mixture was acidified with HCl (2 N) and extracted with ethyl acetate. The organic phase was separated, dried over anhydrous $MgSO_4$, and concentrated *in vacuo* to give the title compound as white powder; ^{1}H NMR (400 MHz, chloroform-*d*) δ 8.12 (t, J = 1.8 Hz, 1H), 7.91 (ddd, J = 7.8, 1.9, 1.1 Hz, 1H), 7.83 (ddd, J = 7.8, 1.9, 1.1 Hz, 1H), 7.64 (t, J = 7.8 Hz, 1H), 7.58−7.51 (m, 2H), 7.25 (d, J = 8.5 Hz, 3H), 7.17 (d, J = 3.5 Hz, 1H), 7.04−6.97 (m, 2H), 6.35 (d, J = 3.5 Hz, 1H), 4.40 (s, 2H), 4.34 (s, 2H), 3.10 (s, 3H), 2.66 (s, 6H), 2.33 (s, 3H); ^{13}C NMR (100 MHz, chloroform-*d*) δ (ppm) 161.9, 155.7, 143.5, 143.3, 142.3, 141.4, 140.6, 138.9, 135.6, 132.7, 132.4, 132.3, 130.1, 129.8, 127.7, 126.2, 126.0, 120.9, 111.9, 50.4, 44.7, 41.8, 23.0, 21.2; HRMS calculated for $C_{29}H_{29}NO_7S_2$ $(M + H)^+$ 568.1458, found 568.1452.

Cell Lines. HEK293 cells were maintained in Dulbecco's modified Eagle's medium supplemented with 10% FBS and antibiotics (penicillin and streptomycin; Invitrogen). HepG2 cells were maintained in minimal essential medium supplemented with 10% FBS and antibiotics.

Transfection Assays. Twenty-four hours prior to transfection, HEK293 cells were seeded in 96-well plates at density of 15×10^3 cells per well, n = 4 (Day 1). Transfections were performed using Lipofectamine 2000 (Invitrogen; Day 2). Twenty-four hours after the transfection, the cells were treated with vehicle or compound and incubated at 37 °C for another twenty-four hours (Day 3). Luciferase activity was measured using the Dual-Glo luciferase assay system (Promega) and analyzed using GraphPad Prism software (Day 4). Data were normalized to Renilla luciferase activity.

Induction of Lipogenesis in Cultured HepG2 Cells. Cells were seeded at 6×10^4 cells per well in polylysine-coated 6-well dishes and allowed to grow to 80% confluency. Once confluency was determined, new media containing 10 μg/mL insulin was added to the cells. Cells were grown in the insulin-containing media for 8 days, with a media change every 2 days.

Animals and Preparation of Tissue Samples. Twenty-one-week-old male C57BL6 DIO mice were purchased from Jackson Laboratories. All procedures were approved and conducted in accordance to the Scripps Florida Institutional Animal Use Committee. Animals were individually housed and fed a high fat diet (60% kcal/fat diet, 20% carbohydrate) for the duration of the experiment that included SR9238 administration for 30 days (30 mg/kg, qd, ip). Prior to initiation of the experiment, animals were provided the high fat diet for 10-weeks. Animals were acclimated to the environment for one week and sham dosed with vehicle for 3 days prior to SR9238 administration. Body weight and food intake was monitored daily. Pre- and postexperiment body composition analysis was performed on all the mice by DEXA. Blood was collected by cardiac puncture and used for plasma cholesterol and triglyceride measurements. Livers were weighed and immediately flash-frozen in liquid nitrogen for gene expression analysis or put in formalin on ice for histology.

Quantitative Real Time PCR. RNA was isolated from HepG2 cells using the Qiagen RNeasy kit or from mouse tissues by Trizol preparation (Invitrogen). Total RNA was reverse transcribed using the iScript cDNA kit (BioRad). qRT-PCR analysis was performed using the SYBR green kit (Roche) with a 7900HT Fast Real Time PCR System (Applied Biosystems). Each sample was run in duplicate and the results were analyzed according to the ddCt method. For HepG2 cells, *cyclophillin B* was used as the reference gene. For mouse tissue, *Gapdh* was used as the reference gene.

	Human
hABCA1 F	5′-AGACGACCACCATGTCAATC-3′
hABCA1 R	5′-CGAATGTCTTTTCCCAGGATG-3′
hcyclophilin F	5′-GCAAATTCCATCGTGTAATCAAG-3′
hcyclophilin R	5′-CGTAGATGCTCTTTCCTCCTG-3′
hFAS F	5′-ACAGGGACAACCTGGAGTTCT-3′
hFAS R	5′-CTGTGGTCCCACTTGATGAGT-3′
hLXRa F	5′-GGAGGTACAACCCTGGGAGT-3′
hLXRa R	5′-AGCAATGAGCAAGGCAAACT-3′
hLXRb F	5′-ATCAAGAGGCCGCAGGACCA-3′
hLXRb R	5′-AGGCGAAGACCTGCTCCGAG-3′
hSREBP-1C F	5′-GGAGGGGTAGGGCCAACGGCCT-3′
hSREBP-1C R	5′-CATGTCTTCGAAAGTGCAATCC-3′
	Mouse
mABCA1 F	5′-GGACATGCACAAGGTCCTGA-3′
mABCA1 R	5′-CAGAAAATCCTGGAGCTTCAAA-3′
mFASN F	5′-GCACAGCTCTGCACTGTCTACTAC-3′
mFASN R	5′-ATCCCAGAGGAAGTCAGATGATAG-3′
mGAPDH F	5′-GCCAAGGCTGTGGGCAAGGT-3′
mGAPDH R	5′-TCTCCAGGCGGCACGTCAGA-3′
mIL-1b F	5′-GCAACTGTTCCTGAACTCA-3′
mIL-1b R	5′-CTCGGAGCCTGTAGTGCAG-3′
mLXRa F	5′-TGCCATCAGCATCTTCTCTG-3′
mLXRa R	5′-GGCTCACCAGCTTCATTAGC-3′
mLXRb F	5′-CGCTACAACCACGAGACAGA-3′
mLXRb R	5′-TGTTGATGGCGATAAGCAAG-3′
mSCD1 F	5′-GGAGACCCCTTAGATCGAGTG-3′
mSCD1 R	5′-CACTCGAATTACTTCCCACCA-3′
mSREBP1c F	5′-TGCTCCTGTGTGATCTACTTCTTG-3′
mSREBP1c R	5′-TGTAGGAATACCCTCCTCATAGCA-3′
mTNFa F	5′-TCAGCCGATTTGCTATCTCAT-3′
mTNFa R	5′-TGGAAGACTCCTCCCAGGTAT-3′

dx.doi.org/10.1021/cb300541g | *ACS Chem. Biol.* 2013, 8, 559−567

Primers. Histology. Liver from DIO mice was allowed to fix overnight at 4 °C in formalin, and then stored in 20% sucrose in PBS solution at 4 °C until cryoprotected. The tissues were then embedded in OCT compound and snap frozen on 100% ethanol with dry ice prior to sectioning. Ten μm sections were stained for lipids with 2 μg/mL Bodipy 493/503 (Molecular Probes) in 1X PBS and counterstained with 1.5 μg/mL DAPI in mounting media (Vector Laboratories). For F4/80 staining, three 10 μm liver sections were added to each well of a 12-well cell culture plate and rinsed three times with 1X PBS. Sections were blocked at RT for 1 h in a 5% NGS, 2% BSA, 0.2% TritonX-100 solution. Alexafluor-488 F4/80 antibody (Abd Serotec) was diluted 1:1000 in blocking solution. Sections were incubated with the antibody at 4 °C overnight, rinsed three times with 1X PBS and mounted onto slides using DAPI mounting media (Vector Laboratories). Lipid droplet and Kupffer cell fluorescence were analyzed using ImageJ public domain software (National Institutes of Health, Bethesda, MD).

Biochemical NR−Cofactor Peptide Interaction Assay (TR-FRET) Assay. Purified human LXRα-LBD (GST), LXRβ-LBD (GST), fluoroscein (FL)-labeled peptides, terbium (TB)-labeled anti-GST tag antibody, and all buffers were purchased from Invitrogen. All LXR assays were conducted in 384-well black medium-binding polystyrene assay plates, n = 4 (Greiner Bio-One). Test compound stock solutions and subsequent serial dilutions were prepared at 100X the final concentration in DMSO, and then were diluted to the final assay concentration of 2X in assay buffer and dispensed into assay plates. LXR-LBDs were added to assay plates and then a mixture of FL-peptide/TB-anti-GST was added to each well containing either a test compound or DMSO control for final concentrations of 2.5nM LXRα-LBD, 5nM LXRβ-LBD, 10 nM TB-anti-GST, and 250 nM FL-peptide. Assay plates were protected from light and incubated with gentle shaking for 3.5 h at RT. The TR-FRET ratio (520 nm/492 nm) of each assay well was measured using the Perkin-Elmer EnVision plate reader. An excitation filter at 340 nm was used to excite the TB-anti-GST and emission filters 492 nm and 520 nm were used to detect terbium and fluorescein emission signals respectively. A delay of 100 μs followed by a 200 μs integration time was used to collect the time-resolved emission signals. NCoR ID1 Sequence: Fluorescein-LITLADHICQIITQ, NCoR ID2 Sequence: Fluorescein-NLGLEDIIRKALMG, and Trap220/Drip-2 Sequence: Fluorescein-NTKNHPMLMNLLKDNPAQD (Invitrogen).

SREBP2 Translocation Assay. HepG2 cells were seeded at 5×10^5 cells/mL in a 4-chamber culture slide (BD Falcon). The following day the media was removed and replaced with antibiotic-free media containing 10 μM of DMSO or SR9238 and cells were allowed to grow for 48 h. Cells were washed in TBS, fixed and fluorescently stained for SREBP2 according to the assay protocol (Caymen Chemicals).

■ ASSOCIATED CONTENT

Ⓢ Supporting Information

This material is available free of charge *via* the Internet at http://pubs.acs.org

■ AUTHOR INFORMATION

Corresponding Author

*E-mail: tburris@scripps.edu.

Notes

The authors declare no competing financial interest.

■ REFERENCES

(1) Browning, J. D., Szczepaniak, L. S., Dobbins, R., Nuremberg, P., Horton, J. D., Cohen, J. C., Grundy, S. M., and Hobbs, H. H. (2004) Prevalence of hepatic steatosis in an urban population in the United States: impact of ethnicity. *Hepatology 40*, 1387−1395.

(2) Szczepaniak, L. S., Nurenberg, P., Leonard, D., Browning, J. D., Reingold, J. S., Grundy, S., Hobbs, H. H., and Dobbins, R. L. (2005) Magnetic resonance spectroscopy to measure hepatic triglyceride content: prevalence of hepatic steatosis in the general population. *Am. J. Physiol. Endocrinol. Metab. 288*, E462−468.

(3) Adams, L. A., and Angulo, P. (2006) Treatment of non-alcoholic fatty liver disease. *Postgrad. Med. J. 82*, 315−322.

(4) Browning, J. D., and Horton, J. D. (2004) Molecular mediators of hepatic steatosis and liver injury. *J. Clin. Invest. 114*, 147−152.

(5) Cohen, J. C., Horton, J. D., and Hobbs, H. H. (2011) Human fatty liver disease: old questions and new insights. *Science 332*, 1519−1523.

(6) Calkin, A. C., and Tontonoz, P. (2012) Transcriptional integration of metabolism by the nuclear sterol-activated receptors LXR and FXR. *Nat. Rev. Mol. Cell. Biol. 13*, 213−224.

(7) Uyeda, K., and Repa, J. J. (2006) Carbohydrate response element binding protein, ChREBP, a transcription factor coupling hepatic glucose utilization and lipid synthesis. *Cell Metab. 4*, 107−110.

(8) Yoshikawa, T., Shimano, H., Amemiya-Kudo, M., Yahagi, N., Hasty, A. H., Matsuzaka, T., Okazaki, H., Tamura, Y., Iizuka, Y., Ohashi, K., Osuga, J., Harada, K., Gotoda, T., Kimura, S., Ishibashi, S., and Yamada, N. (2001) Identification of liver X receptor-retinoid X receptor as an activator of the sterol regulatory element-binding protein 1c gene promoter. *Mol. Cell. Biol. 21*, 2991−3000.

(9) Joseph, S. B., Laffitte, B. A., Patel, P. H., Watson, M. A., Matsukuma, K. E., Walczak, R., Collins, J. L., Osborne, T. F., and Tontonoz, P. (2002) Direct and indirect mechanisms for regulation of fatty acid synthase gene expression by liver X receptors. *J. Biol. Chem. 277*, 11019−11025.

(10) Repa, J. J., Liang, G., Ou, J., Bashmakov, Y., Lobaccaro, J. M., Shimomura, I., Shan, B., Brown, M. S., Goldstein, J. L., and Mangelsdorf, D. J. (2000) Regulation of mouse sterol regulatory element-binding protein-1c gene (SREBP-1c) by oxysterol receptors, LXRalpha and LXRbeta. *Genes Dev. 14*, 2819−2830.

(11) Lima-Cabello, E., Garcia-Mediavilla, M. V., Miquilena-Colina, M. E., Vargas-Castrillon, J., Lozano-Rodriguez, T., Fernandez-Bermejo, M., Olcoz, J. L., Gonzalez-Gallego, J., Garcia-Monzon, C., and Sanchez-Campos, S. (2011) Enhanced expression of pro-inflammatory mediators and liver X-receptor-regulated lipogenic genes in non-alcoholic fatty liver disease and hepatitis C. *Clin. Sci. 120*, 239−250.

(12) Michael, L. F., Schkeryantz, J. M., and Burris, T. P. (2005) The pharmacology of LXR. *Mini Rev. Med. Chem. 5*, 729−740.

(13) Zuercher, W. J., Buckholz, R. G., Campobasso, N., Collins, J. L., Galardi, C. M., Gampe, R. T., Hyatt, S. M., Merrihew, S. L., Moore, J. T., Oplinger, J. A., Reid, P. R., Spearing, P. K., Stanley, T. B., Stewart, E. L., and Willson, T. M. (2010) Discovery of tertiary sulfonamides as potent liver X receptor antagonists. *J. Med. Chem. 53*, 3412−3416.

(14) Naik, S. U., Wang, X., Da Silva, J. S., Jaye, M., Macphee, C. H., Reilly, M. P., Billheimer, J. T., Rothblat, G. H., and Rader, D. J. (2006) Pharmacological activation of liver X receptors promotes reverse cholesterol transport in vivo. *Circulation 113*, 90−97.

(15) Zanotti, I., Poti, F., Pedrelli, M., Bellosta, S., Favari, E., and Bernini, F. (2006) The liver-X-receptor agonist T0901317 stimulates in vivo reverse cholesterol transport in mice. *Arterioscler., Thromb., Vasc., Biol. 26*, E54−E54.

(16) Zhang, Y., Breevoort, S. R., Angdisen, J., Fu, M., Schmidt, D. R., Holmstrom, S. R., Kliewer, S. A., Mangelsdorf, D. J., and Schulman, I. G. (2012) Liver LXRalpha expression is crucial for whole body cholesterol homeostasis and reverse cholesterol transport in mice. *J. Clin. Invest. 122*, 1688−1699.

(17) Gramlich, T., Kleiner, D. E., McCullough, A. J., Matteoni, C. A., Boparai, N., and Younossi, Z. M. (2004) Pathologic features associated with fibrosis in nonalcoholic fatty liver disease. *Hum. Pathol. 35*, 196−199.

(18) McCullough, A. J. (2004) The clinical features, diagnosis and natural history of nonalcoholic fatty liver disease. *Clin. Liver Dis. 8*, 521−533.

(19) Tosello-Trampont, A.-C., Landes, S. G., Nguyen, V., Novobrantseva, T. I., and Hahn, Y. S. (2012) Kupffer cells trigger nonalcholic steatohepatitis development in diet-indiced model through TNF-α production. *J. Biol. Chem. 287*, 40161−40172.

(20) Fernandez-Veledo, S., Nieto-Vazquez, I., Rondinone, C. M., and Lorenzo, M. (2006) Liver X receptor agonists ameliorate TNF alpha-induced insulin resistance in murine brown adipocytes by down-regulating protein tyrosine phosphatase-1B gene expression. *Diabetologia 49*, 3038−3048.

(21) Wang, H., Zhang, Y., Yehuda-Shnaidman, E., Medvedev, A. V., Kumar, N., Daniel, K. W., Robidoux, J., Czech, M. P., Mangelsdorf, D. J., and Collins, S. (2008) Liver X receptor alpha is a transcriptional repressor of the uncoupling protein 1 gene and the brown fat phenotype. *Mol. Cell. Biol. 28*, 2187−2200.
(22) Korach-Andre, M., Archer, A., Barros, R. P., Parini, P., and Gustafsson, J. A. (2011) Both liver-X receptor (LXR) isoforms control energy expenditure by regulating brown adipose tissue activity. *Proc. Natl. Acad. Sci. U.S.A. 108*, 403−408.
(23) Joseph, S. B., Castrillo, A., Laffitte, B. A., Mangelsdorf, D. J., and Tontonoz, P. (2003) Reciprocal regulation of inflammation and lipid metabolism by liver X receptors. *Nat. Med. 9*, 213−219.
(24) Zelcer, N., and Tontonoz, P. (2006) Liver X receptors as integrators of metabolic and inflammatory signaling. *J. Clin. Invest. 116*, 607−614.
(25) Lehmann, J. M., Kliewer, S. A., Moore, L. B., SmithOliver, T. A., Oliver, B. B., Su, J. L., Sundseth, S. S., Winegar, D. A., Blanchard, D. E., Spencer, T. A., and Willson, T. M. (1997) Activation of the nuclear receptor LXR by oxysterols defines a new hormone response pathway. *J. Biol. Chem. 272*, 3137−3140.
(26) Peet, D. J., Turley, S. D., Ma, W., Janowski, B. A., Lobaccaro, J. M., Hammer, R. E., and Mangelsdorf, D. J. (1998) Cholesterol and bile acid metabolism are impaired in mice lacking the nuclear oxysterol receptor LXR alpha. *Cell 93*, 693−704.
(27) Alberti, S., Schuster, G., Parini, P., Feltkamp, D., Diczfalusy, U., Rudling, M., Angelin, B., Bjorkhem, I., Pettersson, S., and Gustafsson, J. A. (2001) Hepatic cholesterol metabolism and resistance to dietary cholesterol in LXRbeta-deficient mice. *J. Clin. Invest. 107*, 565−573.
(28) Schultz, J. R., Tu, H., Luk, A., Repa, J. J., Medina, J. C., Li, L. P., Schwendner, S., Wang, S., Thoolen, M., Mangelsdorf, D. J., Lustig, K. D., and Shan, B. (2000) Role of LXRs in control of lipogenesis. *Genes Dev. 14*, 2831−2838.
(29) Brown, M. S., and Goldstein, J. L. (1997) The SREBP pathway: regulation of cholesterol metabolism by proteolysis of a membrane-bound transcription factor. *Cell 89*, 331−340.
(30) Jeon, T. I., and Osborne, T. F. (2012) SREBPs: metabolic integrators in physiology and metabolism. *Trends Endocrinol Metab 23*, 65−72.